frontiers | Frontiers in Oncology

TYPE Original Research
PUBLISHED 17 August 2023
DOI 10.3389/fonc.2023.1193708



OPEN ACCESS

EDITED BY
Marina Pinheiro,
Chemistry and Technology Network (REQUIMTE), Portugal

REVIEWED BY
Zahra Hosseini-khah,
Mazandaran University of Medical Sciences, Iran
Danijela M. Cvetković,
University of Kragujevac, Serbia

*CORRESPONDENCE
Nosratollah Zarghami
zarghami@tbzmed.ac.ir

†These authors have contributed equally to this work

RECEIVED 25 March 2023
ACCEPTED 13 July 2023
PUBLISHED 17 August 2023

CITATION
Salmani-Javan E, Jafari-Gharabaghlou D, Bonabi E and Zarghami N (2023) Fabricating niosomal-PEG nanoparticles co-loaded with metformin and silibinin for effective treatment of human lung cancer cells.
*Front. Oncol.* 13:1193708.
doi: 10.3389/fonc.2023.1193708



# Fabricating niosomal-PEG nanoparticles co-loaded with metformin and silibinin for effective treatment of human lung cancer cells

Elnaz Salmani-Javan[1†], Davoud Jafari-Gharabaghlou[1†], Esat Bonabi[2] and Nosratollah Zarghami[1,3*]

[1]Department of Clinical Biochemistry and Laboratory Medicine, Faculty of Medicine, Tabriz University of Medical Sciences, Tabriz, Iran, [2]Department of Medical Microbiology, Faculty of Medicine, Istanbul Aydin University, Istanbul, Türkiye, [3]Department of Medical Biochemistry, Faculty of Medicine, Istanbul Aydin University, Istanbul, Türkiye

**Background:** Despite current therapies, lung cancer remains a global issue and requires the creation of novel treatment methods. Recent research has shown that biguanides such as metformin (MET) and silibinin (SIL) have a potential anticancer effect. As a consequence, the effectiveness of MET and SIL in combination against lung cancer cells was investigated in this study to develop an effective and novel treatment method.

**Methods:** Niosomal nanoparticles were synthesized via the thin-film hydration method, and field emission scanning electron microscopy (FE-SEM), Fourier transform infrared (FTIR), atomic force microscopy (AFM), and dynamic light scattering (DLS) techniques were used to evaluate their physico-chemical characteristics. The cytotoxic effects of free and drug-loaded nanoparticles (NPs), as well as their combination, on A549 cells were assessed using the MTT assay. An apoptosis test was used while under the influence of medication to identify the molecular mechanisms behind programmed cell death. With the use of a cell cycle test, it was determined whether pharmaceutical effects caused the cell cycle to stop progressing. Additionally, the qRT-PCR technique was used to evaluate the levels of hTERT, BAX, and BCL-2 gene expression after 48-h medication treatment.

**Results:** In the cytotoxicity assay, the growth of A549 lung cancer cells was inhibited by both MET and SIL. Compared to the individual therapies, the combination of MET and SIL dramatically and synergistically decreased the IC50 values of MET and SIL in lung cancer cells. Furthermore, the combination of MET and SIL produced lower IC50 values and a better anti-proliferative effect on A549 lung cancer cells. Real-time PCR results showed that the expression levels of hTERT and BCL-2 were significantly reduced in lung cancer cell lines treated with MET and SIL compared to single treatments ($p < 0.001$).

**Conclusion:** It is anticipated that the use of nano-niosomal-formed MET and SIL would improve lung cancer treatment outcomes and improve the therapeutic efficiency of lung cancer cells.

KEYWORDS

niosomal nanoparticles, metformin, silibinin, lung cancer, hTERT

# 1 Introduction

In the last century, the most prevalent malignancy is lung cancer, which causes the most mortality from cancers (1). Statistical analysis revealed that lung cancer caused 19% of cancer deaths (2). According to the biology, prognosis, and therapy responsiveness of lung cancer, the World Health Organization (WHO) has categorized it into two groups: small cell lung cancer (SCLC) and non-small cell lung cancer (NSCLC) (3). Almost 85% of types of lung cancer are of the last group (4). Lung cancer has a high prevalence in both men and women (5), but in most countries, men have higher mortality from lung cancer causes (6). Risk factors such as smoking genetics, diet, alcohol, ionizing radiation, air pollution (2), and behavioral and environmental factors (1) are causes of lung cancer (1). However, smoking is considered the most significant risk factor (2). Traditional chemotherapy is limited because of its adverse effects and high cytotoxicity; as a result, the development of another treatment could limit the side effects of the treatment (7). Recent studies recommend a combination of two or more therapeutic compounds to decrease adverse side effects, elevate the modality of life, decrease drug resistance and population of cancer stem cells, reduce metastasis, and improve the lifetime of patients (7, 8). A recent study has shown that the treatment of human colorectal cancer cell lines with metformin (MET) and silibinin (SIL) inhibits cell survival and induces apoptosis (7). SIL is a polyphenolic flavonolignan and natural antioxidant found in *Silybum marianum*. It has anticancer effects in certain cancer forms, like breast, prostate, kidney, skin, pancreas, bladder, lung, and colon cancers. It also has hepato-protective, immune-stimulatory, cell cycle arrest, and antioxidant effects (9, 10) and causes apoptosis activation in various cancer cells (11). SIL exerts anticancer influence through several signaling pathways and molecules including VEGF, VEGF receptors, NF-kB, IGF-IGFBP3, b-catenin, PI3K/Akt, STAT, AMPK, and MAPK [9]. MET is another natural antioxidant that is being applied to manage type 2 diabetes (12, 13). The anticancer effect of MET is mediated by AMPK (13). Also, MET modulates the AMPK/mTOR/p70S6K pathway; inhibits protein synthesis (8, 14), cell mitosis, and proliferation (15, 16); and suppresses metastasis (17). Current studies have shown that in a dose-dependent manner, MET and SIL can suppress the expression of the human telomerase reverse transcriptase (hTERT) gene (18, 19). hTERT gene expression regulates telomerase function (20), produces the telomerase catalytic subunit (21), and keeps the length of the telomere (20, 22). It has been found that telomerase is activated in almost 85%–90% of the most prevalent tumor including pancreatic, prostate, liver, breast, colon, and lung cancers (3, 23). Accordingly, telomerase has been considered a potential treatment target for treating different types of cancers (8, 24, 25). The latest studies have identified BAX and BCL-2 as other genes that influence the survival of cancer cells (26). Bcl-2 is considered a vital regulator and inhibitor of apoptosis (27, 28). It has been revealed that during apoptosis, the expression of BAX is upregulated, the expression of BCL-2 is downregulated, and the ratio of BAX/BCL-2 seems to be important for inducing apoptosis (28, 29). However, a high level of BCL-2 than BAX causes more susceptibility to apoptosis (28, 29). Injected chemotherapy drugs have several insufficiencies including severe side effects, low bioactivity, drug resistance, quick degradation, and clearance from the body. These limitations could be improved using nanoparticles (NPs) as their drug delivery system (30, 31). Different nanoparticles are used in drug delivery, but among them, niosome has been identified as one of the most suitable carriers (32). Niosome is a degradable, biocompatible, non-immunogenic, and harmless carrier composed of non-ionic surfactants and lipid compounds, which could transfer hydrophilic and hydrophobic drugs. Unlike conventional drug delivery forms, the release rate of niosome could be controlled by modifying its composition or surface (33, 34). Polyethylene glycol (PEG) has been approved as a safe surface modifier due to its being biocompatible, hydrophilic, flexible, and non-toxic effects (35). To increase circulatory stability and half-life, niosome could be covered with PEG to form PEGylated niosome. Regarding the anticancer effect of MET and SIL, in this research, we investigate the synergistic effect of co-delivery MET and SIL loaded in PEGylated niosome to enhance their bioavailability and evaluate their effects on the expression of hTERT, BCL-2, and BAX genes in NSCLC type lung cancer cells.

# 2 Material and methods

## 2.1 Cell line and chemicals

A549 lung cancer cell line and human embryonic kidney 293 (HEK 293) were acquired from the Institut Pasteur Cell Bank, Iran (Cat. No C203), and maintained according to recommendations. Metformin (1,1-dimethyl biguanide hydrochloride), silibinin, dimethyl sulfoxide, 3-(4,5-dimethylthiazol-2-yl)-2,5-diphenyltetrazolium bromide (MTT), PEG (Mw = 4,000),

dimethyl sulfoxide (DMSO), polyvinyl alcohol (PVA) and cholesterol, non-ionic surfactants (Span-60), methanol, and chloroform were purchased from Sigma Aldrich (St. Louis, MO, USA). Fetal bovine serum (FBS), penicillin–streptomycin, and RPMI-1640 were taken from Gibco BRL (Gaithersburg, MD, USA). The first strand of complementary DNA (cDNA) synthesized with the kit purchased from Fermentas (Vilnius, Lithuania) and Syber Green PCR Master Mix kit was provided from Roche (Mannheim, Germany).

## 2.2 Metformin- and silibinin-loaded PEGylated-niosome synthesis

First, PEG (3 mg), cholesterol (6 mg), and Span-60 (36 mg) were dissolved in 10 ml of an ethanol/chloroform mixture. The solvent was evaporated using a rotary evaporator at 120 rpm and 60°C under reduced pressure. After the evaporation of the organic solvent, a thin film was formed at the bottom of the round-bottom flask. Then, the formed layer was hydrated with phosphate-buffered saline (PBS) containing MET (1.6 mg) and evaporated by a rotary evaporator at 90 rpm and 60°C. The obtained solvent was collected and sonicated using a sonicator for 30 min to get a uniform, smaller, and more homogenized niosome. To provide SIL-loaded PEGylated niosome, SIL (4.8 mg) was dissolved in a mixture of chloroform–ethanol with niosome. The samples were prepared and kept at 4°C for later analyses.

## 2.3 Size and zeta potential assessments

Dynamic light scattering (DLS) technique (Nano ZS, Malvern Instruments Ltd., Malvern, UK) was applied to evaluate the average size and surface charge of the prepared niosome. In summary, the niosome samples were properly diluted (1:10) with deionized water, and the sample size and zeta potential were measured according to the DLS method using Zetasizer Nano ZS (Malvern Instruments Ltd., Malvern, UK) with a helium–neon laser at 630 nm in room temperature.

## 2.4 FE-SEM

A field emission scanning electron microscopy (FE-SEM) model AIS 2100 (Seron Technologies, Gyeonggi-do, Korea) was used to examine the surface morphology and microstructure of synthesized PEGylated niosome. A small number of samples were used for this, which were rinsed twice with pure water, freeze-dried, and scanned using an electron microscope.

## 2.5 Determination of entrapment efficiency

Spectrophotometry was applied to evaluate the entrapment efficacy (EE). Initially, various doses of MET and SIL in methanol were used to adjust the calibration curve. After that, Amicon MPS (Millipore, Burlington, MA, USA) was used to load a niosome solution and centrifuged (Hettich, Tuttlingen, Germany). The entrapped niosome remained at the top of the tube membrane, while the supernatant was detached from the bottom filter cup. The concentration of free MET and free SIL in the supernatant was recorded using absorbance measurements at 234 and 287 nm, respectively. The percentage of entrapment efficiency was calculated by the following formula:

$$\text{EE\%} = \frac{\text{Total amount of MET/SIL} - \text{free MET/SIL}}{\text{Total amount of MET/SIL}} \times 100.$$

## 2.6 FTIR analysis

In order to distinguish between the loaded and unloaded drug in the niosome, Fourier transform infrared spectroscopy (FTIR) was used. After lyophilized into a dry powder, the samples were combined with potassium bromide. The specimens were then put into a hydraulic press to create pellets. The samples were scanned in the wavelength range of 400–4,000 $cm^{-1}$.

## 2.7 Cell culture

A549 and HEK 293 cell lines were purchased from the Institut Pasteur cell culture collection (Tehran, Iran). The cells were grown in RPMI-1640 medium complemented with FBS (10%), 0.05 mg/ml of penicillin G, and 0.08 mg/ml of streptomycin. Cells were placed in a sterile flask and incubated at 37°C in a humidified atmosphere containing 5% $CO_2$.

## 2.8 Investigation of *in vitro* drug release

With the use of a dialysis bag (MW = 12 kDa), the *in vitro* release of MET and SIL from the niosome was assessed. A specified volume of MET-NP and SIL-NP was dispersed in PBS with pH values of 4.4 and 7.4, respectively. The release of both drugs was estimated in PBS while continuously agitating the MET and SIL niosome samples in the dialysis tubes. After that, the sample was periodically removed from the incubation medium and quickly replaced with an equivalent amount of fresh PBS. A UV–Vis spectrometer was applied to measure the release of MET and SIL at 234 and 287 nm, respectively.

## 2.9 Cytotoxic test

With the use of MTT assay, the cytotoxic properties of drugs were evaluated in their free, loaded, and combination forms. In summary, a 96-well plate was seeded with $2 \times 10^4$ A549 lung cancer cells per well and incubated for 24 h at 37°C in a humidified atmosphere containing 5% $CO_2$ to encourage cell adhesion. Furthermore, we applied human embryonic kidney 293 (HEK 293) as a normal cell line and evaluated the cytotoxicity of

niosomal metformin and silibinin on this cell line. Then, the cells were exposed to various doses of the free and loaded forms of MET and SIL and their combinations listed in Table 1 for 48 h. Also, a group of cells was treated with a blank niosome as a control. Following the incubation period, 200 µl of the phosphate buffer solution containing 0.5 mg/ml of MTT was added to the cell culture wells, and the plates were then covered with an aluminum foil and incubated for 4 h at 37°C. After the addition of 200 µl of pure DMSO and 25 µl of Sorensen's glycine buffer, the entire contents of the wells were then removed. The resulting formazan crystals were then extracted after 20 min of incubation. Finally, using an ELISA microplate reader (BioTek Power Wave XS) with a reference wavelength of 630 nm, the absorbance of formazan at 570 nm was measured, and the number of living cells was evaluated. There were three separate runs of each experiment.

## 2.10 RNA extraction, cDNA synthesis, and real-time PCR

A real-time PCR test was applied to assess the transcription mRNA of hTERT, BAX, and BCL-2 genes. First, $2 \times 10^6$ A549 cells were seeded in six-well plates and incubated at 37°C with 5% $CO_2$. After 24 h, cells were exposed separately to free-MET (F-MET), free-SIL (F-SIL), nano-MET (N-MET), nano-SIL (N-SIL), and a combination of F-MET-SIL and N-MET-SIL at their IC50 concentration. After 48-h treatment of free and drug-loaded NPs, total mRNA was extracted by TRIzol (Sigma, Roedermark, Germany) reagent based on the instrument. Then, using measurements of the OD260/280 ratio, the quantity and quality of the total extracted mRNA were determined. Then, employing a first-strand cDNA synthesis kit (Fermentas, Vilnius, Lithuania), cDNA was synthesized from mRNA extracted from each sample in accordance with the manufacturer's instruction. According to the manufacturer's recommendations, hTERT, BAX, and BCL-2 gene expression levels were then assessed using the qPCR method employing the Hot Taq EvaGreen qPCR. The primer-blast on the National Center for Biotechnology Information (NCBI) website was used to blast the exact primers that were utilized for real-time PCR (Table 2). The program for real-time PCR was as follows; the first step was denaturation at 95°C for 10 min, followed by cycles of denaturation at 95°C for 15 s (1 cycle), annealing step at 60°C for 30 s (40 cycles), extension step at 72°C for 30 s (40 cycles), and melting step at 65°C–95°C (1 cycle). In the end, the housekeeping gene (GAPDH) was used to normalize the relative expression levels of hTERT, BAX, and BCL-2.

## 2.11 Apoptosis analysis

Apoptosis induction was investigated by F-MET, F-SIL, N-MET, N-SIL, and their combination on the A549 cell line using a flow cytometer and Annexin V staining method. In summary, six-well plates containing $5 \times 10^5$ A549 cells were used to treat drugs in free form and nano-form and their combination. After 48 h of drug treatment, cells were harvested using trypsin (Sigma, Germany) and washed three times with PBS solution. Then, a certain amount of fixed solution was used to fix the cells. Annexin, V-FITC, and propidium iodide (PI) were then used to stain the cells, and they were incubated for 20 min. A flow cytometer was used to measure the cell mortality rate.

## 2.12 Cell cycle analysis

A total of $5 \times 10^5$ A549 cells were seeded per well of six-well plates and incubated for 24 h. Then, cells were treated with F-MET, F-SIL, N-MET, N-SIL, and their combinations. Following 48 h of

TABLE 1 Amounts of each compound used for cytotoxicity test.

| SIL (µM) | MET | SIL (µM)/MET (mM) | SIL-NPs (µM) | MET-NPs (µM) | SIL/MET-NPs (µM) |
|---|---|---|---|---|---|
| 5 | 5 | 5/5 | 5 | 25 | 5/25 |
| 10 | 10 | 10/10 | 10 | 50 | 10/50 |
| 15 | 15 | 15/15 | 15 | 100 | 15/100 |
| 30 | 30 | 30/30 | 30 | 150 | 30/150 |
| 40 | 40 | 40/40 | 40 | 200 | 40/200 |

MET, metformin; SIL, silibinin; NPs, nanoparticles.

TABLE 2 Primer sequences used for real-time PCR amplification.

| Genes | Forward (5′→3′) | Reverse (5′→3′) |
|---|---|---|
| hTERT | TTCCTGCACTGGCTGATGAGT | AGAAAGACCTGAGCAGCTCGAC |
| BAX | ACGTGGGCATTTTTCTTACTTT | TATTACCCCCTCAAGACCACT |
| BCL-2 | AAACTTGACAGAGGATCATGC | ATCTTTATTTCATGAGGCACGTT |
| GAPDH | TCTGACTTCAACAGCGACACC | AAATGAGCTTGACAAAGTGGT |

drug exposure, the cells were collected and washed three times with PBS before being fixed with 70% ethanol and stored at −20°C for 48 h. The cells were taken, re-suspended in PBS, and stained with a solution that contains RNase A and PI; then, the cells were incubated for 30 min at 37°C. The fluorescence was read using the flow cytometer.

## 2.13 Statistical analysis

Statistical significance and multi-group comparison of data were performed using a two-way analysis of variance (ANOVA) followed by Tukey's *post-hoc* test using GraphPad Prism (version 8). Results with $p \leq 0.05$ were regarded as statistically significant and were represented as the mean ± standard deviation (SD). All experimental trials were conducted three times and reported as mean ± SD.

# 3 Results and discussion

## 3.1 Size, morphology, and drug loading

According to guidelines, which is a key method for creating therapeutic NPs, MET and SIL were loaded in niosome NPs (36, 37). In cancer treatment, the combination of chemotherapy agents is the first line of cancer treatment. However, due to low stability and unwanted side effects (such as damage to intact cells, hair loss, loss of appetite, diarrhea, and drug resistance), combination chemotherapy is limited. NPs open up new possibilities for cancer treatment (38). The improvement of the bioavailability of drugs that are poorly water-soluble, the co-delivery of two or more drugs, the combination of therapeutic agents, targeted drug delivery, and particularly the accumulation of drugs at the site of the tumor (39), and controlling the release of drugs in target site are all possible with NPs (40). NPs are nano-sized, and for this reason, they can deeply penetrate objective tissues and be taken up by target cells (38). Niosome is a novel NP in the drug delivery system with considerable possibilities in numerous drug delivery systems (41, 42). Bilayer spherical vesicles called niosomes are formed of cholesterol and non-ionic surfactants in an aqueous medium. Cholesterol increases the stability and decreases vesicle permeability, increasing the effectiveness of the drug's encapsulation (41). Because the drug carried in the niosome exclusively targets the intended cell and not non-target cells, the drug dose and toxicity can be minimized. By delaying the removal of medication molecules from circulation, niosomes enhance the therapeutic potential of drugs (42). Applying PEGylation in NPs is one of the most effective and extensively researched methods for enhancing the effectiveness of medications. The use of PEG in nano-formulations gives the nanoparticles hidden qualities, decreases the probability of removal by the reticuloendothelial system, and enhances the bioavailability and half-life of the medication utilized in the formulation (23, 43). PEGylation of the niosome increases their bioavailability. PEGylated niosomes slowly release drugs and can be hidden from the immune system; thus, they can circulate longer in the bloodstream. Additionally, it has been hypothesized that PEG's high hydrophilicity causes niosomes to attach a coating of water to their surface, which hinders macrophages from recognizing and removing them. This change ultimately gives the niosomes more time *in vivo* to find their target sites before being digested by macrophages (44). To assess particle size and NP dispersion, the DLS method was used. As mentioned in Table 3, PEGylated niosome represented an average size of 124 ± 7.8 nm with a uniform size distribution, a polydispersity index (PDI) of 0.561, and zeta potential of −7.64 ± 4.2 mV. The average sizes of PEGylated-N-MET and PEGylated-N-SIL were 139 ± 4.1 and 147 ± 7.2 nm, respectively, with PDI of 0.912 and 0.596, respectively, and zeta potential of −24.37 ± 2.9 and −9.86 ± 3.7 mV, respectively. The size of N-MET and N-SIL was bigger than that of PEGylated niosome, which inferred that drugs were successfully loaded in NPs. PEGylated-N-MET-SIL displayed the largest size with 162.5 ± 1.8 nm (Figure 1A). The PDI of PEGylated-N-MET-SIL in comparison with N-MET and N-SIL due to the co-loading of MET and SIL was low, which led to the formation of the well-knit structures of the NPs. For the synthesized NPs, an average surface charge between −7.64 and −17.7 was found (Figure 1B). Smaller mean diameter NPs essentially migrate more quickly than bigger NPs in a known applied electric field. As a result, they have higher zeta potential values, which increases the stability of NPs in colloidal dispersion (45, 46).

The SEM technique was used to examine the morphology of drug-loaded PEGylated-niosome NPs. The images of N-MET and N-SIL revealed an average diameter of approximately 145 nm and confirmed the drug's spherical form and identical dispersion, which is shown in Figure 2.

According to the atomic force microscopy (AFM) analysis findings (Figure 3), which are in agreement with the SEM image and estimated size, particles with a height of approximately 66.7 nm from the surface are thought to be made of N-MET-SIL. Due to the use of a dehydrated sample of N-MET-SIL during the photography process, the size indicated by AFM was smaller than the results given by the DLS method.

TABLE 3 Characterization of PEGylated-niosome and drug-loaded NPs using DLS.

| Groups | Size (nm) | Polydispersity index | Zeta potential (mV) |
|---|---|---|---|
| **PEGylated niosome** | 124 ± 7.8 | 0.561 | −7.64 ± 4.2 |
| **MET-PEGylated niosome** | 139 ± 4.1 | 0.912 | −24.37 ± 2.9 |
| **SIL-PEGylated niosome** | 147 ± 7.2 | 0.596 | −9.86 ± 3.7 |
| **MET-SIL-PEGylated Niosome** | 162.5 ± 1.8 | 0.424 | −17.7 ± 7 |

NPs, nanoparticles; DLS, dynamic light scattering; MET, metformin; SIL, silibinin.

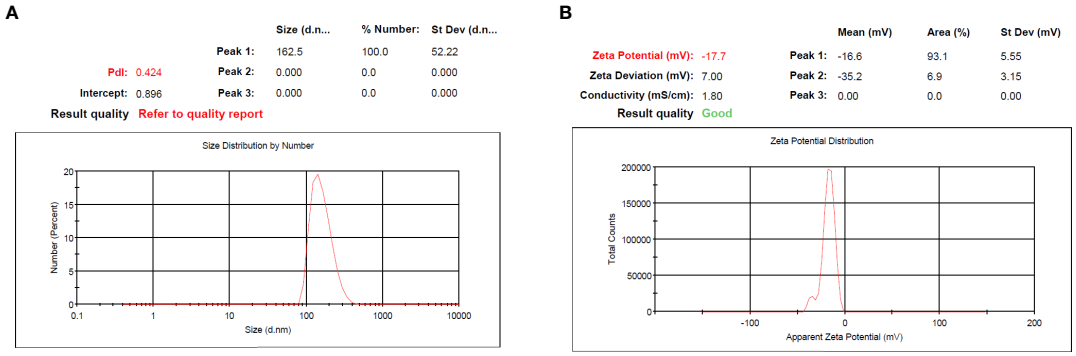


FIGURE 1
**(A)** PDI and **(B)** zeta potential of PEGylated-N-MET-SIL. PDI, polydispersity index; MET, metformin; SIL, silibinin.

The drug encapsulation efficiency range was approximately 88.6%. To demonstrate the structure of F-MET and F-SIL and N-MET-SIL, FTIR spectroscopy was used (Figure 4). The FTIR spectrum of F-MET demonstrated two broad peaks at 3,300–3,600 $cm^{-1}$ assigned to O–H and N–H bands, respectively, of polymer and drug. The peak at 2,362 $cm^{-1}$ was related to MET C═N of imines stretching vibration. The peak at 2,362 $cm^{-1}$ was related to MET C═N of imines stretching vibration. An intense peak at 1,759 $cm^{-1}$ was the characteristic esoteric (O–C═O) bands of PEGylated niosome section. The peaks at 1,508–1,669 $cm^{-1}$ are characteristic bands of NH primary bending, NH secondary bending, and C–N stretching vibrations of MET. Other characteristic peaks of –MET, which indicated C–C, C–O, and C–O–C, appeared at 1,059–1,187 $cm^{-1}$. The FTIR spectrum of F-SIL showed a peak at 2,885 $cm^{-1}$ attributed to C–H stretch of CH, and 3,010 and 2,955 $cm^{-1}$ are due to C–H stretch of CH. A sharp peak at 1,630 $cm^{-1}$ is attributed to C–O stretch. Absorption at 1,186–1,089.6 $cm^{-1}$ is assigned to C–O stretch. The results display that MET and SIL have been successfully combined with PEGylated-niosome NPs. Our data were in agreement with the findings of Soumaye Amirsaadat et al. (47).

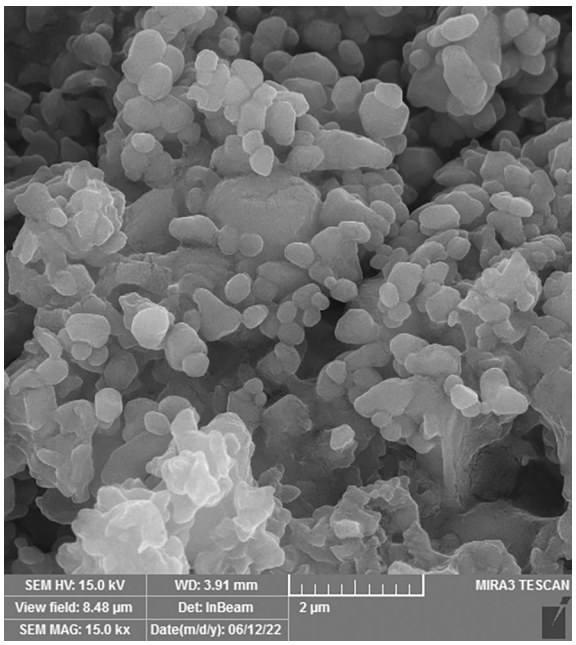


FIGURE 2
Field emission scanning electron microscopy (FE-SEM) analysis of PEGylated-N-MET-N-SIL displaying the core-shell structure of NPs. NPs, nanoparticles; MET, metformin; SIL, silibinin.

## 3.2 Drug release analysis

*In vitro*, drug release analyses were performed by using the dialysis method at pH of 7.4 and 4.4 (48). The cumulative proportion of MET and SIL released from NPs during various time periods is displayed in Figure 5.

Release of MET-NP and SIL-NP occurred in two phases. Initially, a controlled release was carried out for 6 h at a burst drug release rate, allowing for the release of 25% of the entrapped MET and SIL. After that, a continuous phase was carried out for 120 h at a reduced and slow release rate, and the maximum release of MET and SIL from PEGylated niosome reached 50% and 40% of the total entrapped drug, respectively, which indicated that persistency of MET and SIL in niosome at pH 7.4 is acceptable. This two-phase release pattern is in accordance with previous observations and seems to be a characteristic of bilayer vesicles in general (49).

## 3.3 *In vitro* cytotoxicity and synergistic analysis

The MTT test is one of the best techniques to evaluate the cytotoxic effects of drugs on cell proliferation (48). After 48-h drug treatment, an MTT test was performed to estimate the synergistic inhibitory and cytotoxic properties of MET and SIL in free form and nano-form and their combination. According to recent research, combining chemotherapeutic medicines rather than using them separately may be more effective at preventing the growth of tumors and lowering drug toxicity. With this strategy, drug resistance and ineffective drug use can be reduced, and therapeutic medication effectiveness can be increased (50). Our results demonstrated that

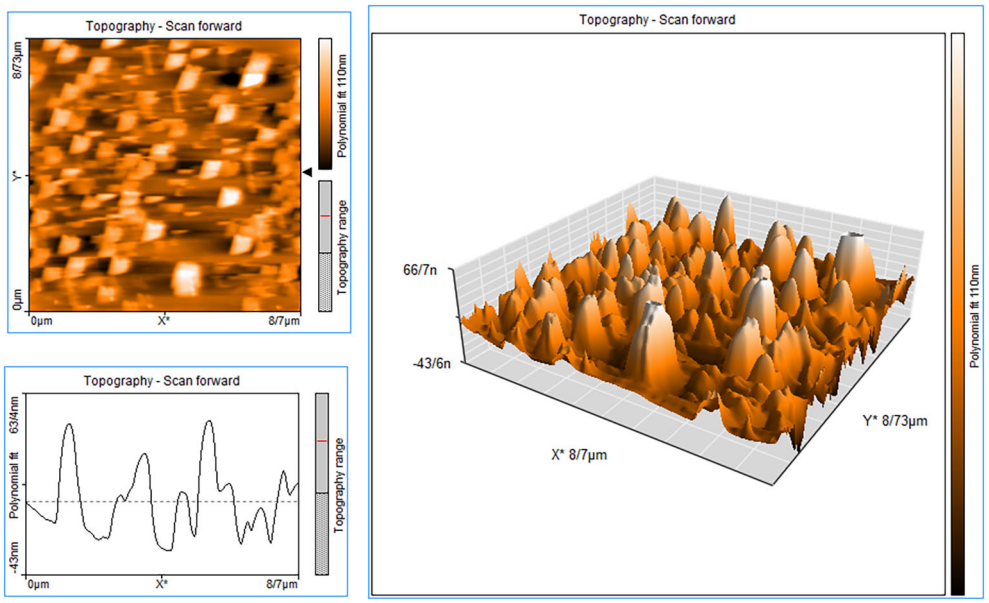


FIGURE 3
AFM image of N-MET-SIL indicated surface morphology of drug-loaded NPs. AFM, atomic force microscopy; NPs, nanoparticles; MET, metformin; SIL, silibinin.

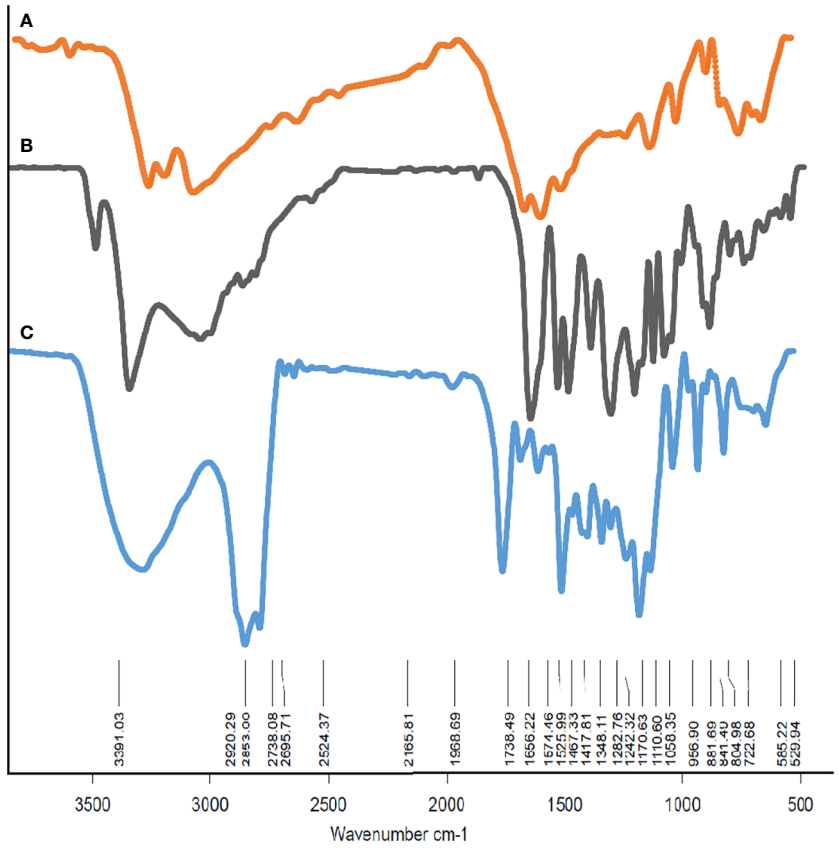


FIGURE 4
The FTIR spectrum of **(A)** F-MET, **(B)** F-SIL, and **(C)** PEGylated niosomal loaded MET-SIL. FTIR, Fourier transform infrared; MET, metformin; SIL, silibinin.

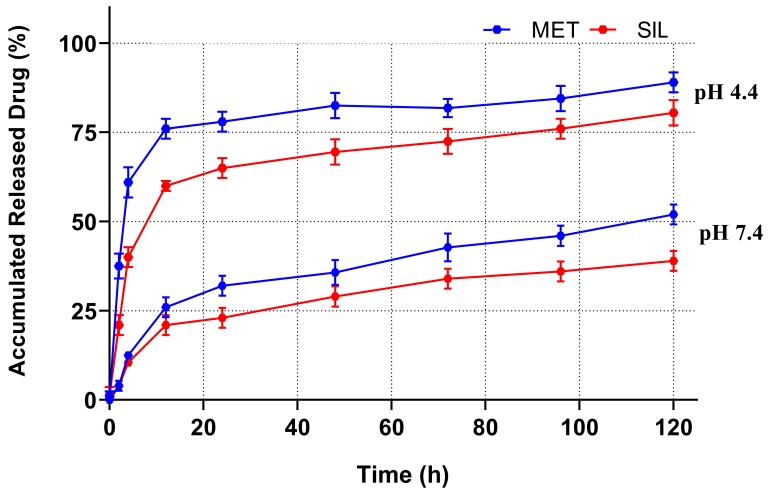


FIGURE 5
Drug release patterns of MET and SIL released from PEGylated-N-MET-SIL in PBS solution at pH 7.4 and 4.4. PBS, phosphate-buffered saline; MET, metformin; SIL, silibinin.

MET and SIL could inhibit the growth and development of A549 cells, but the combination of MET/SIL niosome and F-MET/SIL had greater synergistic effects in comparison to the individual agents. These combinations were also able to conquer the toxicity and other side effects of a single agent and significantly suppress the development of the A549 cell line in a time- and dose-dependent manner (51). The blank niosome does not show any significant effect on the cells even in high doses. According to the result of the MTT assay, the blank niosome treatment group was excluded from the rest of the tests.

As shown in Figure 6, due to delayed release and improved drug absorption from the niosome, the cytotoxic effects of medicines in N-MET and N-SIL are greater than F-MET and F-SIL in the A549 cell line. Moreover, the treatment of HEK 293 cells with the applied

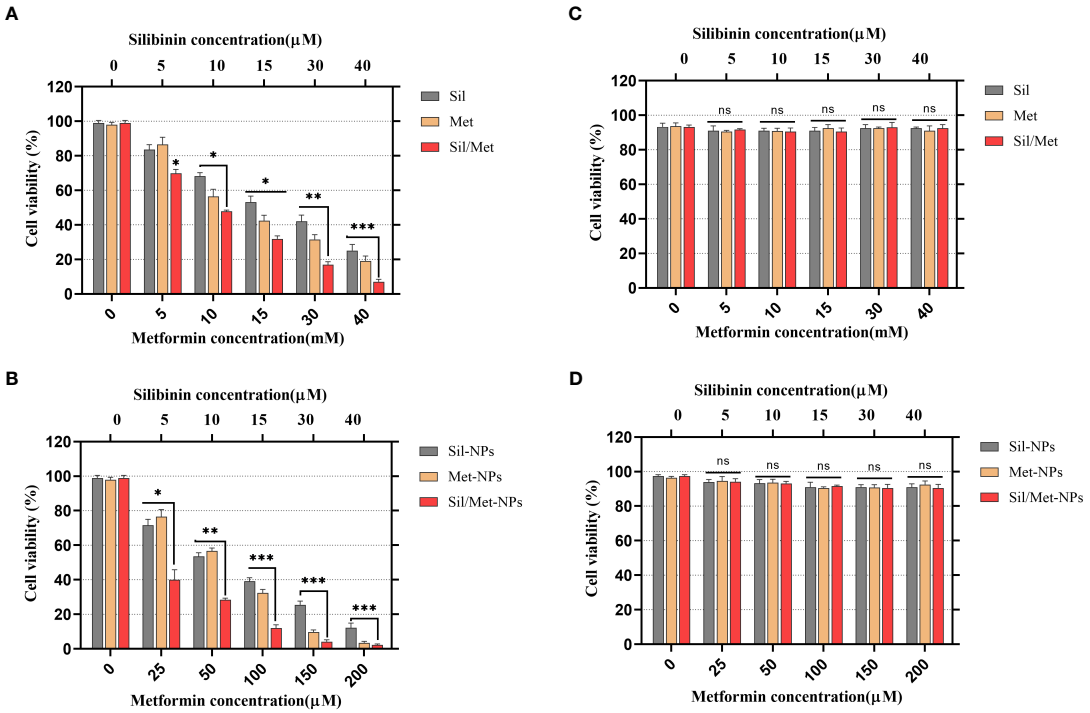


FIGURE 6
Effects of MET, SIL, and their nano-form on A549 lung cancer cell viability. **(A)** A549 cell line was treated with F-MET and F-SIL and their combination. **(B)** A549 cell line was treated with PEGylated-N-MET, PEGylated-N-SIL, and their combination. **(C)** HEk-293 cell line was treated with F-MET and F-SIL and their combination. **(D)** HEk-293 cell line treatment with PEGylated-N-MET, PEGylated-N-SIL, and their combination. Cell viability was measured using MTT assay after 48-h treatment. Data represented are from three independent experiments (***p< 0.001, **p< 0.01, and *p< 0.05). MET, metformin; SIL, silibinin; and ns, not significant.

agents demonstrated no significant cytotoxicity. It suggests that by improving MET's and SIL's solubility and bioavailability, this form of drug delivery system could enhance its transport to cancer cells (48). The findings of our investigation are in agreement with those of former research that has shown that MET and SIL inhibit the growth and proliferation of the A549 cell line (52–54).

IC50 and combination index (CI50) values for pharmaceutical formulation against A549 cells after 48 h of incubation are shown in Table 4, which indicated that N-MET/SIL remarkably have lower IC50 at 48 h. The median-effect approach was used to assess the exact nature of the interaction between MET and SIL in combination form, where CL values greater than, equal to, or less than 1 suggest antagonism, additivity, or synergism effects in the medication combination, respectively (8). The combination of F-MET/SIL and N-MET-SIL had a synergistic influence against A549 cell growth, as shown by the CI50s of F-MET/SIL and N-MET/SIL determined by the combination index chart to be 0.5236 and 0.3409, respectively (Figure 7). However, N-MET-SIL has higher synergistic effects against the development of A549 cells.

Dose effect evaluation of F-MET, F-SIL, N-MET, N-SIL, and their combination indicated that drugs in combination form have a greater effect than a single form. Moreover, our results showed that the combination of MET and SIL in the niosome has a higher effect on the A549 cell line as shown in Figure 8.

## 3.4 Real-time PCR

To examine the anticancer effects of MET and SIL in free and encapsulation forms and their combination in the A549 cell line, the transcription levels of hTERT, BAX, and BCL-2 genes were measured by RT-PCR.

BAX (pro-apoptotic) and BCL-2 (anti-apoptotic) belong to the BCL-2 family, which regulates the apoptosis process through the mitochondrial pathway (55). A recent study has shown that normal expression of BAX in cancer cells was associated with better results, while expression of BCL-2 in tumor cells caused drug resistance. Therefore, it is anticipated that altering the expression of these genes will cause apoptosis and prevent the growth of cancer cells (56).

Abnormal expression of telomerase is found in many cancers that have an essential role in the proliferation and immortality of tumor cells, which is a hallmark of cancer cells. This feature of telomerase becomes a potential target in cancer treatment and drug delivery (57). It is believed that hTERT's transcriptional modulation, which activates telomerase in a variety of malignancies, is essential. Also, it has been demonstrated that inhibiting hTERT stimulates the activation of apoptosis in cancer cells (47). As a result, discovering a treatment that can both suppress gene expression and trigger apoptosis may be a useful first step in treating lung cancer.

In our research, it is found that MET and SIL in free and nano-capsulated forms inhibited the expression of hTERT and BCL-2 while inducing the expression of BAX (Figure 9).

Also, our results have discovered that F-MET/SIL and N-MET/SIL downregulate hTERT and BCL-2 and upregulate BAX more than individual forms. This proves that drug combination may enhance anticancer effects and have a synergistic inhibitory impact on tumor cells. This approach could be helpful to increase the therapeutic benefit of individual treatment, particularly in the elimination of obstacles such as tumor resistance and low drug efficiency. Our data are in agreement with those of a recent study that has shown that MET and SIL alone and in combination could inhibit hTERT gene expression (58).

TABLE 4 IC50 and combination index (CI50) values for the drug formulations against A549 and cells for 48-h incubation time.

| Form | Metformin | Silibinin | MET in combination | SIL in combination | CI50 |
|---|---|---|---|---|---|
| **Pure** | 11.95 mM | 28.86 µM | 7.29 mM | 17.36 µM | 0.5236 |
| **Nano** | 68.42 µM | 10.36 µM | 27.34 µM | 8.14 µM | 0.3409 |

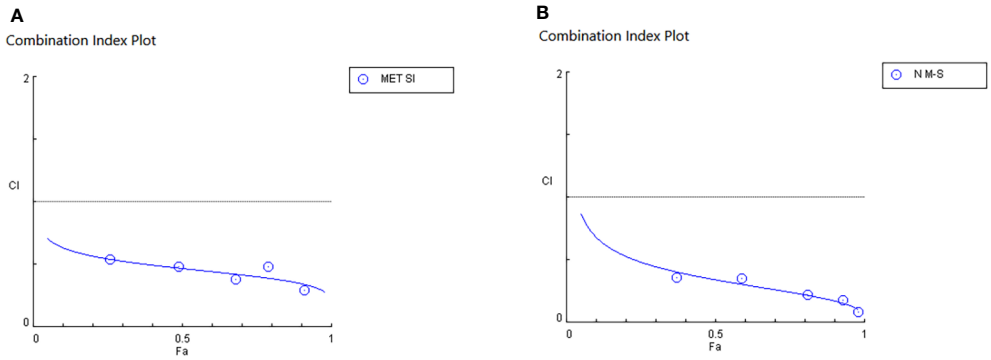


FIGURE 7
Synergistic inhibitory effects of MET and SIL on the growth of A549 cells. **(A)** F-MET/SIL. **(B)** N-MET/SIL. Combination index (CI) was calculated by isobologram analysis using the Chou–Talalay method. CI = 1, additive effect; CI 1, antagonistic effect. Data represented are from three independent experiments. MET, metformin; SIL, silibinin.

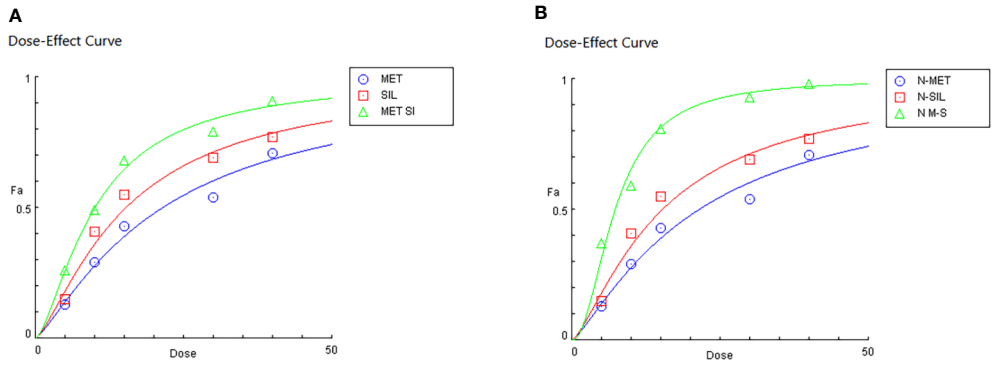


FIGURE 8
Dose effects of MET and SIL in free form **(A)** and nano-form **(B)**. MET, metformin; SIL, silibinin.

## 3.5 Apoptosis

To evaluate the anticancer effect of drugs, an apoptosis assay can be performed (59). Apoptosis is a specifically programmed signaling pathway that induces cell death. Numerous conditions in cancer cells including increased levels of anti-apoptotic proteins and decreased levels of pro-apoptotic proteins cause the apoptotic process to be inhibited, which accelerates cancer cell development and resistance to numerous types of anticancer drugs (60). For this reason, the discovery of treatments that promote the efficient destruction of cancer cells by apoptosis has been one of the clinical oncologists' purposes for more than three decades (61). Herbal remedies exhibit anticancer efficacy through the stimulation of apoptotic pathways, which is regarded as a novel cancer therapy (60). Recent studies demonstrated that MET and SIL induce apoptosis in most cancer cells (62, 63). In this study, we showed the efficacy of F-MET, F-SIL, N-MET, N-SIL, and their combination on induction of apoptosis in A549 lung cancer cells. Our data indicated that both MET and SIL induce apoptosis in the A549 lung cancer cell line. Results demonstrated that MET and SIL in nano-form induce apoptosis more than an individual one. Also, our findings showed that a combination of F-MET/SIL and N-MET/SIL significantly induces apoptosis and causes cell death in the A549 lung cancer cell line, while N-MET-SIL has a greater effect than F-MET-SIL (Figure 10).

In line with our results, Cheng-Chia Tsai et al. have shown that combined treatment of MET and SIL induces apoptosis in colorectal cancer, whereas there was no evidence of apoptosis in colorectal cancer cells when MET and SIL were used alone (7).

## 3.6 Cell cycle

The cell cycle is highly regulated by a group of enzymes, proteins, cytokines, and specific cell cycle signaling pathways, which have a critical role in cellular proliferation and repair processes (64). Continued cell division is a hallmark of cancer cells that is due to mutations that cause damage to cell cycle

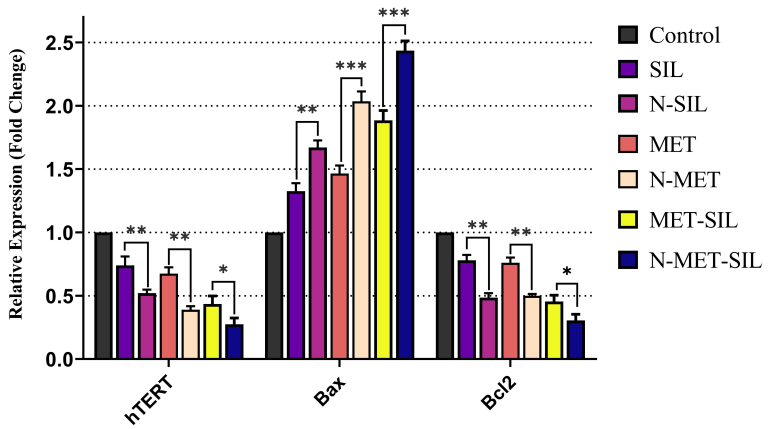


FIGURE 9
Inhibitory effects of F-MET, F-SIL, their nano-form, and their combination on expression levels of hTERT, BAX, and BCL-2 in A549 lung cancer cells. Data represented are from three independent experiments (***p< 0.001, **p< 0.01, and *p< 0.05). MET, metformin; SIL, silibinin.

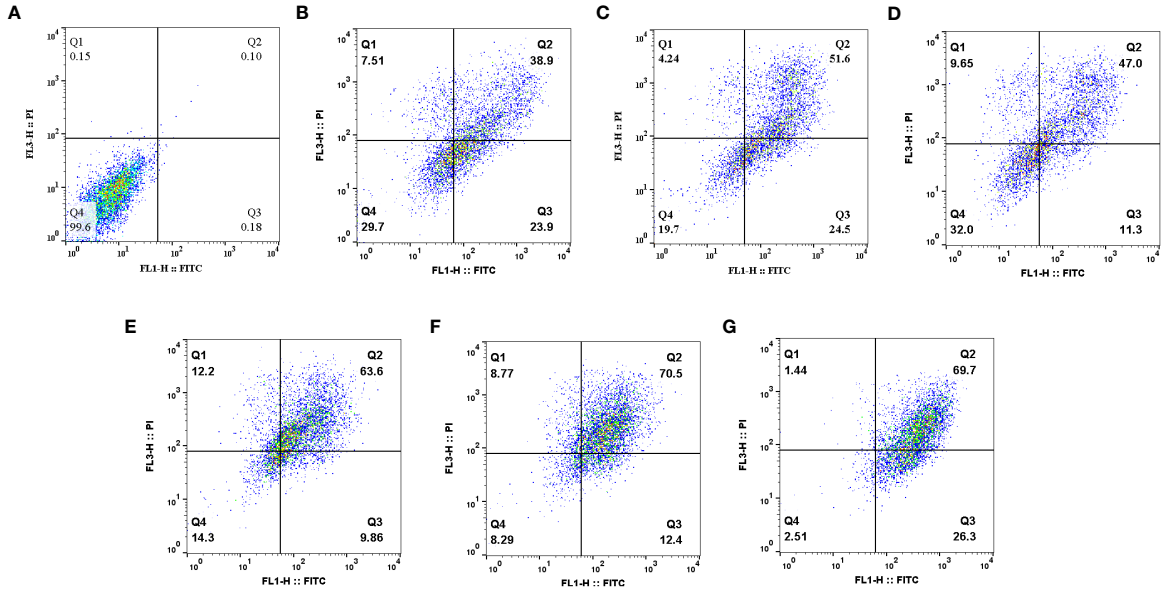


FIGURE 10
Effects of F-MET, F-SIL, N-MET, N-SIL, and their combination on induction of apoptosis in A549 lung cancer cell line. **(A)** Niosome, **(B)** F-MET, **(C)** N-MET, **(D)** F-SIL, **(E)** N-SIL, **(F)** F-MET-SIL, and **(G)** N-MET-SIL. MET, metformin; SIL, silibinin.

regulators and cell cycle progression. A necessary consequence is that all cancer cells are related to the non-stop cell cycle. Understanding the mechanisms of the continuous cell cycle in cancer cells could improve therapeutic opportunities to create new combination treatments (65). Recent studies have shown that MET and SIL could induce cell cycle arrest in most cancer cells (62, 66). Dong Hao Jin et al. indicated that MET could promote cell cycle arrest at the G1 phase of the cell cycle (67). Also, Samiha Mateen et al. demonstrated that SIL suppressed the cell cycle at the G1 phase (68). In this research, we assessed the effect of F-MET, F-SIL, N-MET, N-SIL, and their combination and synergistic effect on the cell cycle of the A549 lung cancer cell line. Our data are in agreement with the previous studies mentioned that MET and SIL could suppress the cell cycle at phase G1, and nano-capsulation of these drugs had a higher effect (Figures 11 and 12). Also, we demonstrated that the combination of MET and SIL and their nano-form significantly suppress the cell cycle at phase G1.

## 4 Conclusion

In this study, we aimed to synthesize an effective delivery system of PEGylated niosome for metformin and silibinin and evaluated their anticancer effect against A549 lung cancer cells.

The anticancer effect of the metformin and silibinin was increased when they were loaded in PEGylated niosomal NPs compared to the free form. This study exhibited that PEGylated niosomal NPs are an appropriate approach for the effective delivery of drugs for lung cancer cells. Metformin and silibinin in free and encapsulated forms induced apoptosis and cell cycle arrest in cancer cell lines. This evidence suggested that applying a combination of drugs in PEGylated niosomal NPs had a greater effect on inducing apoptosis cell cycle arrest. According to the result of qRT-PCR, the expression of hTERT and BCL-2 genes decreased significantly, while the expression of BAX increased in the treated A549 lung cancer cells. In particular, the downregulation of hTERT and BCL-2

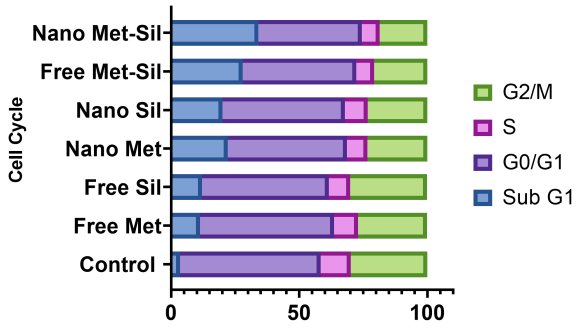


FIGURE 11
Suppression effects of MET and SIL, their nano-form and their combination on cell cycle of A549 cell line.

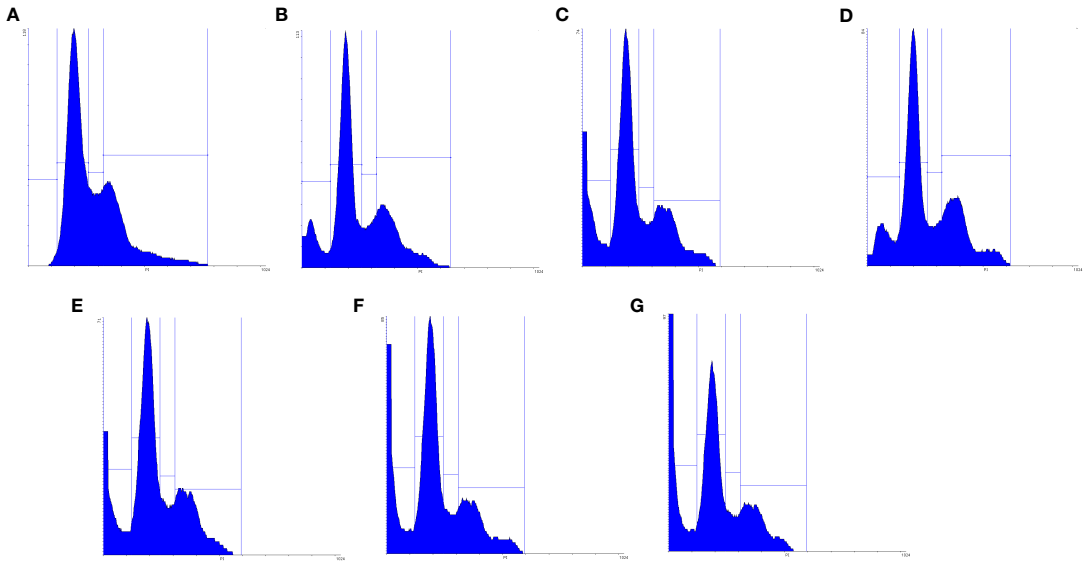


FIGURE 12
Schematic figure of MET, SIL, F-MET, F-SIL and their combination on cell cycle arrest of A549 cell line. **(A)** Niosome, **(B)** F-MET, **(C)** N-MET, **(D)** F-SIL, **(E)** N-SIL, **(F)** F-MET-SIL, **(G)** N-MET-SIL.

and upregulation of BAX gene expression were enhanced when cells treated with the combination of metformin and silibinin were loaded into PEGylated niosomal NPs. Finally, it can be determined that a combination of metformin and silibinin in PEGylated niosomal NPs is an effective strategy for treating lung cancer, and future studies need to investigate the effects of these drugs in *in vivo* experiments.

## Data availability statement

The data that support the findings of this study are available on request from the corresponding author.

## Author contributions

Writing—original draft preparation: ES-J. Editing: DJ-G and EB. Conceptualization and supervision: NZ. All authors contributed to the article and approved the submitted version.

## Acknowledgments

We would like to thank the Tuberculosis and Lung Disease Research Center of Tabriz University of Medical Sciences for all its support (grant No: 62945).

## Conflict of interest

The authors declare that the research was conducted in the absence of any commercial or financial relationships that could be construed as a potential conflict of interest.

## Publisher's note



## References

1. de Groot PM, Wu CC, Carter BW, Munden RF. The epidemiology of lung cancer. *Transl Lung Cancer Res* (2018) 7(3):220–33. doi: 10.21037/tlcr.2018.05.06

2. Malhotra J, Malvezzi M, Negri E, La Vecchia C, Boffetta P. Risk factors for lung cancer worldwide. *Eur Respir J* (2016) 48(3):889–902. doi: 10.1183/13993003.00359-2016

3. Zalewska-Ziob M, Dobija-Kubica K, Biernacki K, Adamek B, Kasperczyk J, Brulinski K, et al. Clinical and prognostic value of hTERT mRNA expression in patients with non-small-cell lung cancer. *Acta Biochim Pol* (2017) 64(4):641–6. doi: 10.18388/abp.2017_1618

4. Cao Z, Gao Q, Fu M, Ni N, Pei Y, Ou WB. Anaplastic lymphoma kinase fusions: Roles in cancer and therapeutic perspectives. *Oncol Lett* (2019) 17(2):2020–30 doi: 10.3892/ol.2018.9856

5. Boloker G, Wang C, Zhang J. Updated statistics of lung and bronchus cancer in United States (2018). *J Thorac Dis* (2018) 10(3):1158–61. doi: 10.21037/jtd.2018.03.15

6. Bray F, Ferlay J, Soerjomataram I, Siegel RL, Torre LA, Jemal A. Global cancer statistics 2018: GLOBOCAN estimates of incidence and mortality worldwide for 36 cancers in 185 countries. *CA Cancer J Clin* (2018) 68(6):394–424. doi: 10.3322/caac.21492

7. Tsai CC, Chuang TW, Chen LJ, Niu HS, Chung KM, Cheng JT, et al. Increase in apoptosis by combination of metformin with silibinin in human colorectal cancer cells. *World J Gastroenterol* (2015) 21(14):4169–77. doi: 10.3748/wjg.v21.i14.4169

8. Jafari-Gharabaghlou D, Pilehvar-Soltanahmadi Y, Dadashpour M, Mota A, Vafajouy-Jamshidi S, Faramarzi L, et al. Combination of metformin and phenformin synergistically inhibits proliferation and hTERT expression in human breast cancer cells. *Iran J Basic Med Sci* (2018) 21(11):1167–73. doi: 10.22038/IJBMS.2018.30460.7345

9. Amirsaadat S, Pilehvar-Soltanahmadi Y, Zarghami F, Alipour S, Ebrahimnezhad Z, Zarghami N. Silibinin-loaded magnetic nanoparticles inhibit hTERT gene expression and proliferation of lung cancer cells. *Artif Cells Nanomed Biotechnol* (2017) 45(8):1649–56. doi: 10.1080/21691401.2016.1276922

10. Imai-Sumida M, Chiyomaru T, Majid S, Saini S, Nip H, Dahiya R, et al. Silibinin suppresses bladder cancer through down-regulation of actin cytoskeleton and PI3K/Akt signaling pathways. *Oncotarget* (2017) 8(54):92032. doi: 10.18632/oncotarget.20734

11. Pashaei-Asl F, Pashaei-Asl R, Khodadadi K, Akbarzadeh A, Ebrahimie E, Pashaiasl M. Enhancement of anticancer activity by silibinin and paclitaxel combination on the ovarian cancer. *Artif Cells Nanomed Biotechnol* (2018) 46 (7):1483–7. doi: 10.1080/21691401.2017.1374281

12. Bailey CJ. Metformin: historical overview. *Diabetologia* (2017) 60(9):1566–76. doi: 10.1007/s00125-017-4318-z

13. Mallik R, Chowdhury TA. Metformin in cancer. *Diabetes Res Clin Pract* (2018) 143:409–19. doi: 10.1016/j.diabres.2018.05.023

14. Sahabi S, Jafari-Gharabaghlou D, Zarghami N. A new insight into cell biological and biochemical changes through aging. *Acta Histochemica* (2022) 124(1):151841. doi: 10.1016/j.acthis.2021.151841

15. Lei Y, Yi Y, Liu Y, Liu X, Keller ET, Qian CN, et al. Metformin targets multiple signaling pathways in cancer. *Chin J Cancer* (2017) 36(1):17. doi: 10.1186/s40880-017-0184-9

16. Khodadadi M, Jafari-Gharabaghlou D, Zarghami N. An update on mode of action of metformin in modulation of meta-inflammation and inflammaging. *Pharmacol Rep* (2022) 74(2):310–22. doi: 10.1007/s43440-021-00334-z

17. Sacco F, Calderone A, Castagnoli L, Cesareni G. The cell-autonomous mechanisms underlying the activity of metformin as an anticancer drug. *Br J Cancer* (2016) 115(12):1451–6. doi: 10.1038/bjc.2016.385

18. Ebrahimnezhad Z, Zarghami N, Keyhani M, Amirsaadat S, Akbarzadeh A, Rahmati M, et al. Inhibition of hTERT gene expression by silibinin-loaded PLGA-PEG-Fe3O4 in T47D breast cancer cell line. *Bioimpacts* (2013) 3(2):67–74.

19. Javidfar S, Pilehvar-Soltanahmadi Y, Farajzadeh R, Lotfi-Attari J, Shafiei-Irannejad V, Hashemi M, et al. The inhibitory effects of nano-encapsulated metformin on growth and hTERT expression in breast cancer cells. *J Drug Deliv Sci Technol* (2018) 43:19–26. doi: 10.1016/j.jddst.2017.09.013

20. Guilleret I, Benhattar J. Demethylation of the human telomerase catalytic subunit (hTERT) gene promoter reduced hTERT expression and telomerase activity and shortened telomeres. *Exp Cell Res* (2003) 289(2):326–34. doi: 10.1016/S0014-4827(03)00281-7

21. Horikawa I, Cable PL, Mazur SJ, Appella E, Afshari CA, Barrett JC. Downstream E-box-mediated regulation of the human telomerase reverse transcriptase (hTERT) gene transcription: evidence for an endogenous mechanism of transcriptional repression. *Mol Biol Cell* (2002) 13(8):2585–97. doi: 10.1091/mbc.e01-11-0107

22. Hassani N, Jafari-Gharabaghlou D, Dadashpour M, Zarghami N. The effect of dual bioactive compounds artemisinin and metformin co-loaded in PLGA-PEG nanoparticles on breast cancer cell lines: potential apoptotic and anti-proliferative action. *Appl Biochem Biotechnol* (2022) 194(10):4930–45. doi: 10.1007/s12010-022-04000-9

23. Mousazadeh H, Pilehvar-Soltanahmadi Y, Dadashpour M, Zarghami N. Cyclodextrin based natural nanostructured carbohydrate polymers as effective non-viral siRNA delivery systems for cancer gene therapy. *J Controlled Release* (2021) 330:1046–70. doi: 10.1016/j.jconrel.2020.11.011

24. Jafari-Gharabaghlou D, Dadashpour M, Khanghah OJ, Salmani-Javan E, Zarghami N. Potentiation of Folate-Functionalized PLGA-PEG nanoparticles loaded with metformin for the treatment of breast Cancer: possible clinical application. *Mol Biol Rep* (2023) 50(4), 1–11. doi: 10.1007/s11033-022-08171-w

25. Amirsaadat S, Jafari-Gharabaghlou D, Dadashpour M, Zarghami N. Potential anti-proliferative effect of nano-formulated curcumin through modulating micro RNA-132, Cyclin D1, and hTERT genes expression in breast cancer cell lines. *J Cluster Sci* (2023) 34, 1–10. doi: 10.1007/s10876-023-02404-z

26. Schuyer M, van der Burg M, Henzen-Logmans S, Fieret J, Klijn J, Look M, et al. Reduced expression of BAX is associated with poor prognosis in patients with epithelial ovarian cancer: a multifactorial analysis of TP53, p21, BAX and BCL-2. *Br J Cancer* (2001) 85(9):1359–67. doi: 10.1054/bjoc.2001.2101

27. Mandal M, Adam L, Mendelsohn J, Kumar R. Nuclear targeting of Bax during apoptosis in human colorectal cancer cells. *Oncogene* (1998) 17(8):999–1007. doi: 10.1038/sj.onc.1202020

28. Zhang G-J, Kimijima I, Onda M, Kanno M, Sato H, Watanabe T, et al. Tamoxifen-induced apoptosis in breast cancer cells relates to down-regulation of bcl-2, but not bax and bcl-XL, without alteration of p53 protein levels. *Clin Cancer Res* (1999) 5(10):2971–7.

29. Choudhuri T, Pal S, Agwarwal ML, Das T, Sa G. Curcumin induces apoptosis in human breast cancer cells through p53-dependent Bax induction. *FEBS Lett* (2002) 512 (1-3):334–40. doi: 10.1016/S0014-5793(02)02292-5

30. Wang H, Zhao Y, Wu Y, Hu YL, Nan K, Nie G, et al. Enhanced anti-tumor efficacy by co-delivery of doxorubicin and paclitaxel with amphiphilic methoxy PEG-PLGA copolymer nanoparticles. *Biomaterials* (2011) 32(32):8281–90. doi: 10.1016/j.biomaterials.2011.07.032

31. Bhargava-Shah A, Foygel K, Devulapally R, Paulmurugan R. Orlistat and antisense-miRNA-loaded PLGA-PEG nanoparticles for enhanced triple negative breast cancer therapy. *Nanomedicine* (2016) 11(3):235–47. doi: 10.2217/nnm.15.193

32. Zinatloo-Ajabshir Z, Zinatloo-Ajabshir S. Preparation and characterization of curcumin niosomal nanoparticles via a simple and eco-friendly route. *J Nanostructures* (2019) 9(4):784–90.

33. De S, Kundu R, Biswas A. Synthesis of gold nanoparticles in niosomes. *J Colloid Interface Sci* (2012) 386(1):9–15. doi: 10.1016/j.jcis.2012.06.073

34. Jadid MFS, Jafari-Gharabaghlou D, Bahrami MK, Bonabi E, Zarghami N. Enhanced anti-cancer effect of curcumin loaded-niosomal nanoparticles in combination with heat-killed Saccharomyces cerevisiae against human colon cancer cells. *J Drug Deliv Sci Technol* (2023) 80, 104167. doi: 10.1016/j.jddst.2023.104167

35. Anari E, Akbarzadeh A, Zarghami N. Chrysin-loaded PLGA-PEG nanoparticles designed for enhanced effect on the breast cancer cell line. *Artif Cells Nanomed Biotechnol* (2016) 44(6):1410–6. doi: 10.3109/21691401.2015.1029633

36. Hasan AA, Madkor H, Wageh S. Formulation and evaluation of metformin hydrochloride-loaded niosomes as controlled release drug delivery system. *Drug Deliv* (2013) 20(3-4):120–6. doi: 10.3109/10717544.2013.779332

37. Amiri B, Ebrahimi-Far M, Saffari Z, Akbarzadeh A, Soleimani E, Chiani M. Preparation, characterization and cytotoxicity of silibinin-containing nanoniosomes in T47D human breast carcinoma cells. *Asian Pacif J Cancer Prev* (2016) 17(8):3835–8.

38. Awasthi R, Roseblade A, Hansbro PM, Rathbone MJ, Dua K, Bebawy M. Nanoparticles in cancer treatment: opportunities and obstacles. *Curr Drug Targets* (2018) 19(14):1696–709. doi: 10.2174/1389450119666180326122831

39. Khan H, Ullah H, Martorell M, Valdes SE, Belwal T, Tejada S, et al. Flavonoids nanoparticles in cancer: Treatment, prevention and clinical prospects. *Semin Cancer Biol* (2021) 69:200–11. doi: 10.1016/j.semcancer.2019.07.023

40. Bajpai S, Tiwary SK, Sonker M, Joshi A, Gupta V, Kumar Y, et al. Recent advances in nanoparticle-based cancer treatment: A review. *ACS Appl Nano Mater* (2021) 4(7):6441–70. doi: 10.1021/acsanm.1c00779

41. Mohamad Saimi NI, Salim N, Ahmad N, Abdulmalek E, Abdul Rahman MB. Aerosolized niosome formulation containing gemcitabine and cisplatin for lung cancer treatment: optimization, characterization and *in vitro* evaluation. *Pharmaceutics* (2021) 13(1), 59. doi: 10.3390/pharmaceutics13010059

42. Joy C, Nair SK, Kumar KK, Dineshkumar B. Niosomes as nano-carrier based targeted drug delivery system. *J Drug Deliv Ther* (2021) 11(4-S):166–70. doi: 10.22270/jddt.v11i4-S.4907

43. Kenechukwu FC, Nnamani DO, Duhu JC, Nmesirionye BU, Momoh MA, Akpa PA, et al. Potential enhancement of metformin hydrochloride in solidified reverse micellar solution-based PEGylated lipid nanoparticles targeting therapeutic efficacy in diabetes treatment. *Heliyon* (2022) 8(3):e09099. doi: 10.1016/j.heliyon.2022.e09099

44. Davarpanah F, Khalili Yazdi A, Barani M, Mirzaei M, Torkzadeh-Mahani M. Magnetic delivery of antitumor carboplatin by using PEGylated-Niosomes. *Daru* (2018) 26, 57–64. doi: 10.1007/s40199-018-0215-3

45. Tavakoli F, Jahanban-Esfahlan R, Seidi K, Jabbari M, Behzadi R, Pilehvar-Soltanahmadi Y, et al. Effects of nano-encapsulated curcumin-chrysin on telomerase, MMPs and TIMPs gene expression in mouse B16F10 melanoma tumour model. *Artif Cells Nanomed Biotechnol* (2018) 46(sup2):75–86. doi: 10.1080/21691401.2018.1452021

46. Shahbazi R, Jafari-Gharabaghlou D, Mirjafary Z, Saeidian H, Zarghami N. Design and optimization various formulations of PEGylated niosomal nanoparticles loaded with phytochemical agents: potential anti-cancer effects against human lung cancer cells. *Pharmacol Rep* (2023) 75(2):442–55. doi: 10.1007/s43440-023-00462-8

47. Amirsaadat S, Jafari-Gharabaghlou D, Alijani S, Mousazadeh H, Dadashpour M, Zarghami N. Metformin and Silibinin co-loaded PLGA-PEG nanoparticles for effective combination therapy against human breast cancer cells. *J Drug Deliv Sci Technol* (2021) 61:102107. doi: 10.1016/j.jddst.2020.102107

48. Mogheri F, Jokar E, Afshin R, Akbari AA, Dadashpour M, Firouzi-amandi A, et al. Co-delivery of metformin and silibinin in dual-drug loaded nanoparticles synergistically improves chemotherapy in human non-small cell lung cancer A549 cells. *J Drug Deliv Sci Technol* (2021) 66:102752. doi: 10.1016/j.jddst.2021.102752

49. El-Ridy MS, Yehia SA, Elsayed I, Younis MM, Abdel-Rahman RF, El-Gamil MA. Metformin hydrochloride and wound healing: from nanoformulation to pharmacological evaluation. *J Liposome Res* (2019) 29(4):343–56. doi: 10.1080/08982104.2018.1556291

50. Thriveni K, Raju A, Kumar RV, Krishnamurthy S, Chaluvarayaswamy R. Patterns of relative telomere length is associated with hTERT gene expression in the tissue of patients with breast cancer. *Clin Breast Cancer* (2019) 19(1):27–34. doi: 10.1016/j.clbc.2018.07.021

51. Salmani Javan E, Lotfi F, Jafari-Gharabaghlou D, Mousazadeh H, Dadashpour M, Zarghami N. Development of a magnetic nanostructure for co-delivery of metformin and silibinin on growth of lung cancer cells: possible action through

leptin gene and its receptor regulation. *Asian Pac J Cancer Prev* (2022) 23(2):519–27. doi: 10.31557/APJCP.2022.23.2.519

52. Morelli AP, Tortelli TCJr., Pavan ICB, Silva FR, Granato DC, Peruca GF, et al. Metformin impairs cisplatin resistance effects in A549 lung cancer cells through mTOR signaling and other metabolic pathways. *Int J Oncol* (2021) 58(6):1–15. doi: 10.3892/ijo.2021.5208

53. Raval M, Patel P, Airao V, Bhatt V, Sheth N. Novel silibinin loaded chitosan-coated PLGA/PCL nanoparticles based inhalation formulations with improved cytotoxicity and bioavailability for lung cancer. *Bionanoscience* (2021) 11(1):67–83. doi: 10.1007/s12668-020-00797-z

54. Mohammadinejad S, Jafari-Gharabaghlou D, Zarghami N. Development of PEGylated PLGA nanoparticles co-loaded with bioactive compounds: potential anticancer effect on breast cancer cell lines. *Asian Pacif J Cancer Prev* (2022) 23 (12):4063–72. doi: 10.31557/APJCP.2022.23.12.4063

55. Flores-Romero H, Hohorst L, John M, Albert MC, King LE, Beckmann L, et al. BCL-2-family protein tBID can act as a BAX-like effector of apoptosis. *EMBO J* (2022) 41(2):e108690. doi: 10.15252/embj.2021108690

56. Pisani C, Ramella M, Boldorini R, Loi G, Billia M, Boccafoschi F, et al. Apoptotic and predictive factors by Bax, Caspases 3/9, Bcl-2, p53 and Ki-67 in prostate cancer after 12 Gy single-dose. *Sci Rep* (2020) 10(1):1–10. doi: 10.1038/s41598-020-64062-9

57. Li Y, Pan G, Chen Y, Yang Q, Hao T, Zhao L, et al. Inhibitor of the human telomerase reverse trancriptase (hTERT) gene promoter induces cell apoptosis via a mitochondrial-dependent pathway. *Eur J Medicinal Chem* (2018) 145:370–8. doi: 10.1016/j.ejmech.2017.12.077

58. Chatran M, Pilehvar-Soltanahmadi Y, Dadashpour M, Faramarzi L, Rasouli S, Jafari-Gharabaghlou D, et al. Synergistic anti-proliferative effects of metformin and silibinin combination on T47D breast cancer cells via hTERT and cyclin D1 inhibition. *Drug Res* (2018) 68(12):710–6. doi: 10.1055/a-0631-8046

59. Gross J, Palmowski K, Doleschel D, Rix A, Gremse F, Verburg F, et al. Change of apoptosis and glucose metabolism in lung cancer xenografts during cytotoxic and anti-angiogenic therapy assessed by annexin V based optical imaging and 18F-FDG-PET/CT. *Contrast Media Mol Imaging* (2021) 2021, 6676337. doi: 10.1155/2021/6676337

60. Pfeffer CM, Singh AT. Apoptosis: a target for anticancer therapy. *Int J Mol Sci* (2018) 19(2):448. doi: 10.3390/ijms19020448

61. Carneiro BA, El-Deiry WS. Targeting apoptosis in cancer therapy. *Nat Rev Clin Oncol* (2020) 17(7):395–417. doi: 10.1038/s41571-020-0341-y

62. Jahanafrooz Z, Motamed N, Rinner B, Mokhtarzadeh A, Baradaran B. Silibinin to improve cancer therapeutic, as an apoptotic inducer, autophagy modulator, cell cycle inhibitor, and microRNAs regulator. *Life Sci* (2018) 213:236–47. doi: 10.1016/j.lfs.2018.10.009

63. Chen Y-H, Yang S-F, Yang C-K, Tsai H-D, Chen T-H, Chou M-C, et al. Metformin induces apoptosis and inhibits migration by activating the AMPK/p53 axis and suppressing PI3K/AKT signaling in human cervical cancer cells. *Mol Med Rep* (2021) 23(1):1–. doi: 10.3892/mmr.2020.11725

64. Sun Y, Liu Y, Ma X, Hu H. The influence of cell cycle regulation on chemotherapy. *Int J Mol Sci* (2021) 22(13):6923. doi: 10.3390/ijms22136923

65. Matthews HK, Bertoli C, de Bruin RA. Cell cycle control in cancer. *Nat Rev Mol Cell Biol* (2022) 23(1):74–88. doi: 10.1038/s41580-021-00404-3

66. Li B, Zhou P, Xu K, Chen T, Jiao J, Wei H, et al. Metformin induces cell cycle arrest, apoptosis and autophagy through ROS/JNK signaling pathway in human osteosarcoma. *Int J Biol Sci* (2020) 16(1):74. doi: 10.7150/ijbs.33787

67. Jin DH, Kim Y, Lee BB, Han J, Kim HK, Shim YM, et al. Metformin induces cell cycle arrest at the G1 phase through E2F8 suppression in lung cancer cells. *Oncotarget* (2017) 8(60):101509. doi: 10.18632/oncotarget.21552

68. Mateen S, Tyagi A, Agarwal C, Singh RP, Agarwal R. Silibinin inhibits human nonsmall cell lung cancer cell growth through cell-cycle arrest by modulating expression and function of key cell-cycle regulators. *Mol Carcinog* (2010) 49(3):247–58. doi: 10.1002/mc.20595